

The path-tracking controller based on dynamic model with slip for one four-wheeled OMR

Yanwen Huang and Qixin Cao

Research Institute of Robotics, Shanghai Jiao Tong University, Shanghai, China, and

Chuntao Leng

School of Mechanical Engineering, Shanghai Jiao Tong University, Shanghai, China

Abstract

Purpose – This paper aims to propose a suitable motion control method for omni-directional mobile robots (OMRs). In RoboCup competition, the robot moves in a dynamic and oppositional environment, which occurs with high acceleration and deceleration motion frequently, especially for our OMR that slipping is almost inherently encountered in motion. Therefore, the purpose of this paper is to present one improved dynamical model with slip, and then to propose one suitable path-tracking controller based on it, which gives more accurate control result.

Design/methodology/approach – A dynamic modeling method for OMRs based on the theory of vehicle dynamics is proposed. By analyzing the wheel contact friction forces both in the wheel hub rolling direction and in the roller rolling direction, an amendatory dynamics model is presented. This model is introduced into the computed-torque-like-controller (CTLC) system to solve the path-tracking problem.

Findings – An amendatory dynamics model with slip is analyzed and introduced into the CTLC system to solve the path tracking problem for OMR in this paper. The anti-disturbance ability and the trajectory tracking effect of the proposed motion control method are proven through simulations and experiments.

Practical implications – The proposed path tracking control method based on one improved dynamic model with slip is applied successfully to achieve effective motion control for one four-wheel OMR, which is suitable for any kind of OMR.

Originality/value – One amendatory dynamics model including slipping between the wheels and ground is presented. Based on the above-slipping model, one CTLC is implemented to solve the path-tracking problem for one four-wheel OMR.

Keywords Friction, Control technology, Robotics, Slip, Controllers

Paper type Research paper

1. Introduction

Wheeled mobile robots have good maneuverability that makes them be applied widely in production and people's daily life. Differential driving is the most common movement. But with the special mechanism of omni-directional wheels, omni-directional mobile robot (OMR) performs 3 degrees-of-freedom (DOFs) motion on the two-dimensional plane, which can achieve translation and rotation simultaneously along arbitrary direction. Using this type of drive system, time is saved by eliminating the need for a robot to rotate before translating from points *A* to *B*. Owing to the more agile performance, OMRs have been applied in many fields, such as omni-directional wheelchairs (Wada, 2005) and in RoboCup competition (He *et al.*, 2004).

Many research groups are paying attention to OMRs (Watanabe *et al.*, 1998; Myung *et al.*, 2000; Witus, 2000).

For example, Watanabe *et al.* (1998) presented state variable-based modeling of a three-wheeled OMR, whose wheels are assumed to be symmetrically arranged orthogonal assemblies. Williams *et al.* (2002a, b) expanded this model to a nonsymmetrical arranged three-wheeled OMR, and the dynamic model of the robot is considered in order to study the slipping effects between the wheels of the vehicle and the working surface. Muir and Neuman (1987a, b) presented the kinematics modeling of four-wheeled mobile robots. Carter *et al.* (2001) described the mechanical design of the OMR and based on its dynamic model proposed a proportional-integral-derivative control for each robot wheel independent of the nonlinear model of the vehicle. From above-existing research results and our experiments, we found that the three-wheeled OMRs may have stability problem due to the triangular contact area with the ground, especially when the location of the center of gravity is high or the size of the robot is small (Pin and Killough, 1994; Muir and Neuman, 1987a, b). Therefore, it is desirable that four-wheeled vehicles will be used when stability is of great concern, for example, in the drastically antagonistic RoboCup competition environment. Therefore, our first task in this paper is to give the design of

The current issue and full text archive of this journal is available at www.emeraldinsight.com/0143-991X.htm



Industrial Robot: An International Journal
37/2 (2010) 193–201
© Emerald Group Publishing Limited [ISSN 0143-991X]
[DOI 10.1108/01439911011018975]

This work is supported by the National High Technology Research and Development Program of China (863 Program), 2007AA041602-1.

one four-wheeled OMR which is used in RoboCup middle-size league competition and, to present a detailed nonlinear dynamics model of the OMR in which both the motor dynamics and robot nonlinear motion dynamics are considered.

However, independent drive of four wheels creates one extra DOF, which requires an accurate control for the robot. Any disturbing or disorder, even temporarily, will cause wheel slippage, while slipping is almost inherently encountered in motion for OMRs. This unexpected behavior motivated the development of a dynamic model including slip. And some researchers realized this. For example, Nobuhiro *et al.* (2007) discussed the tracking control of OMR in consideration of driving wheel slips measured through a two wheels caster, which needs accessional components. Williams *et al.* (2002a, b) presented a dynamic model for OMR, including wheel/motion surface slip and experimentally measured friction coefficients. However, there are few studies on slipping model for one over constrained system of OMRs. Therefore, the main focus of the paper is to present a dynamic model for one four-wheel OMR that includes slipping between the wheels and the motion surface. As one omnidirectional wheel consists of a wheel hub driven by a servo DC motor and rollers that are mounted on the hub rotating passively, our slipping model includes both friction functions in the wheel hub rolling direction and in the roller rolling direction, which is the function of velocity in that direction, respectively.

The path tracking problem is fundamental for more advanced behavior generation. So, this problem has been investigated by many researchers, especially for the nonholonomic wheeled mobile robots. Many of the earlier works addressing the tracking problem were described in Dixon *et al.* (2000), Do *et al.* (2004) and Driessen (2006). However, the trajectory tracking problem of an OMR remains open. Therefore, the third task of this paper is to design a robot path-tracking controller based on the nonlinear dynamical model. Liu *et al.* (2003) designed a controller based on a trajectory linearization strategy for one OMR, but only simulations testing results were shown. Tsai and Wang (2005) proposed an adaptive robust control method for trajectory tracking and path following of a three-wheel OMR via the integral backstepping model, but this method did not consider the issues of the parameter variations and the uncertainties from friction and slip. Chong-Cheng Shing described the design of T-S fuzzy path controller for improving the high-speed tracking accuracy of a four-wheel OMR. The T-S fuzzy model is described by a set of fuzzy “IF [...] THEN” rules, which means that different situation needs different rules (Shing *et al.*, 2006). Vazquez and Velasco-Villa (2007) developed a computed-torque-controller (CTC) strategy to solve the path-tracking problem of a wheeled OMR, assuring the closed loop stability of the system when the state was available for measurement, allowing in this way the convergence of the tracking errors. The CTC is often proposed in order to achieve tracking control of robot manipulators, and it has been shown experimentally that a CTC scheme performs well (de Wit and Roskam, 1991; Sarkar *et al.*, 1994). Following the preliminary research, in this section, we apply the computed-torque-like-controller (CTLIC) strategy to solve the path-tracking control of our four-wheeled OMR.

Therefore, based on the preliminary study result summarized in Cao *et al.* (2007), this work presents the path-tracking controller based on the dynamical model with slip for one four-wheeled OMR, which is organized as follows: in Section 2, the kinematics and dynamics model of the four-wheeled OMR is presented. Based on this model, in Section 3, an amendatory dynamics model with slip between the wheels and the motion surface is developed. In Section 4, path-tracking control system is described based on CTLIC. In Section 5, the proposed strategy is evaluated by means of simulation and real-time hardware test showing its adequate performance and finally, in Section 6, some conclusions are presented.

2. Kinematics and dynamics model of the four-wheeled OMR

This section presents the kinematics and dynamic modeling of a four-wheeled omni-directional robot.

First, we suppose that the robot moves in the plain face. There are two coordinate frames used in this modeling: the body frame, fixed on the moving robot with the origin in the center of gravity of the robot, denoted as $X_R O_R Y_R$, and the world frame, which is fixed on the play ground, denoted as $X_O O_O Y_O$, as shown in Figure 1. Then at any time t , the robot's velocity state can be confirmed by the Cartesian coordinate of the robot in $\{O\}$ and $\{R\}$ as:

$$\dot{\mathbf{X}}_t = \begin{pmatrix} \dot{x}_t & \dot{y}_t & \dot{\theta}_t \end{pmatrix}^T = {}^O_R \mathbf{T} \cdot \mathbf{V}_R = {}^O_R \mathbf{T} \cdot \begin{pmatrix} V_x & V_y & \omega \end{pmatrix}^T \quad (1)$$

where ${}^O_R \mathbf{T}$ is the coordinate transform matrix from the body frame $\{R\}$ to the world frame $\{O\}$ given as:

$${}^O_R \mathbf{T} = \begin{pmatrix} \cos \theta_t & -\sin \theta_t & 0 \\ \sin \theta_t & \cos \theta_t & 0 \\ 0 & 0 & 1 \end{pmatrix} \quad (2)$$

Figure 2 shows a bottom view of our robot. Four wheels are symmetrically mounted on the robot platform with a 90° angle between adjacent wheel rotational axes.

Figure 1 The robot and the world coordinate system

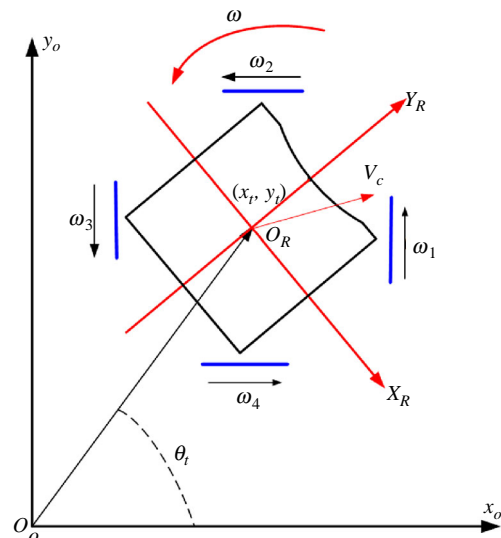
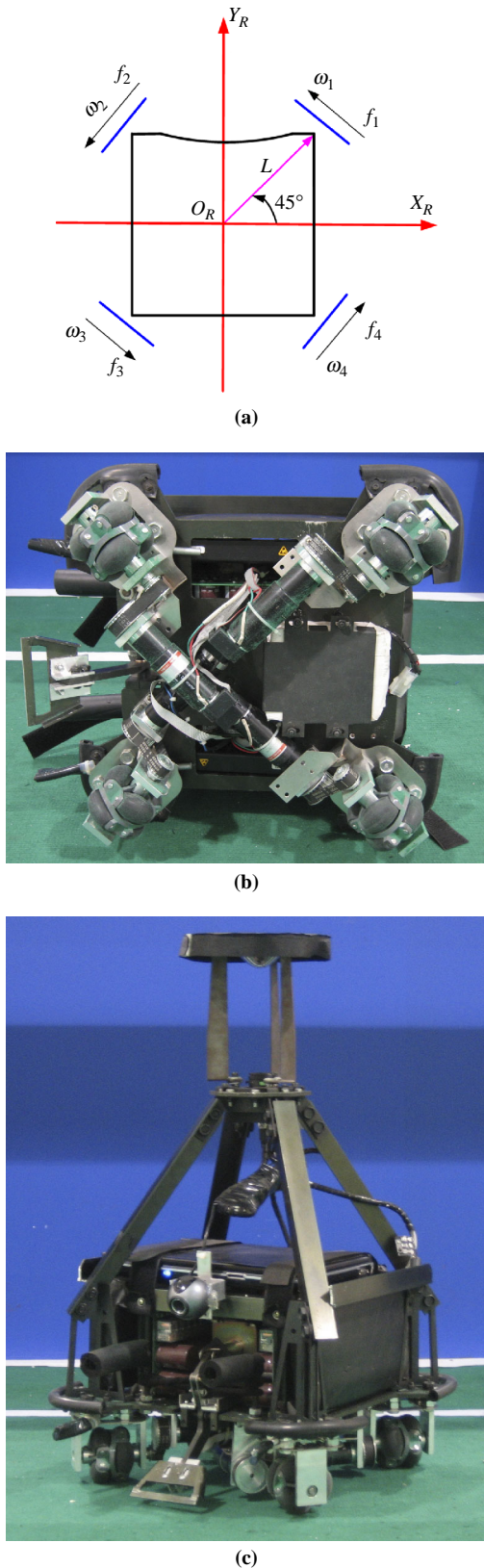


Figure 2



Notes: (a) Arrangement of wheels; (b) bottom view of the four-wheeled OMR; (c) overview of the prototype robot

The nomenclature used in the model is defined as follows:

World frame:

$\mathbf{X} = (x \ y \ \theta)$ Robot location and orientation angle.

Body frame:

$\mathbf{V}_R = (V_x \ V_y \ \omega)$ Velocity and angular rate of the robot in the body frame.

$\mathbf{F} = (f_1 \ f_2 \ f_3 \ f_4)$ Traction force of each wheel.

$\mathbf{\Omega}_m = (\omega_{m1} \ \omega_{m2} \ \omega_{m3} \ \omega_{m4})$ Rotate speed of each motor.

$\mathbf{U} = (u_1 \ u_2 \ u_3 \ u_4)$ Applied armature voltage on each motor.

$\mathbf{F}_\mu = (f_{\mu1} \ f_{\mu2} \ f_{\mu3} \ f_{\mu4})$ Vicious friction force between each wheel and the ground surface.

Mechanical constants:

m = Robot mass.

I_z = Robot moment of inertia.

R = Radius of wheel.

L = Radial distance from the robot center to the wheels.

n = Gear ratio.

2.1 Kinematics modeling

As shown in Figure 2, based on the robot's morphology, it is easy to derive the inverse kinematic equations of the OMR as follows:

$$V_1 = -\frac{\sqrt{2}}{2} \cdot V_x + \frac{\sqrt{2}}{2} \cdot V_y + L \cdot \omega$$

$$V_2 = -\frac{\sqrt{2}}{2} \cdot V_x - \frac{\sqrt{2}}{2} \cdot V_y + L \cdot \omega$$

$$V_3 = \frac{\sqrt{2}}{2} \cdot V_x - \frac{\sqrt{2}}{2} \cdot V_y + L \cdot \omega$$

$$V_4 = \frac{\sqrt{2}}{2} \cdot V_x + \frac{\sqrt{2}}{2} \cdot V_y + L \cdot \omega$$

Which can be simplified as:

$$\mathbf{V}_\omega = \mathbf{J} \cdot \mathbf{V}_R$$

$$\text{where } \mathbf{V}_\omega = [V_1 \ V_2 \ V_3 \ V_4]^T = \left(\frac{R}{n}\right) \cdot \mathbf{\Omega}_m$$

$$\text{and } \mathbf{J} = \begin{pmatrix} -\frac{\sqrt{2}}{2} & \frac{\sqrt{2}}{2} & L \\ -\frac{\sqrt{2}}{2} & -\frac{\sqrt{2}}{2} & L \\ \frac{\sqrt{2}}{2} & -\frac{\sqrt{2}}{2} & L \\ \frac{\sqrt{2}}{2} & \frac{\sqrt{2}}{2} & L \end{pmatrix} \quad (3)$$

2.2 Dynamics modeling

The equation of dynamics for the robot which began with Newton's second law can be written as:

$$m(\dot{V}_x - V_y \cdot \omega) = F_x$$

$$m(\dot{V}_y + V_x \cdot \omega) = F_y \quad (4)$$

$$I_z \cdot \dot{\omega} = M_z$$

Computing the relationship between the robot Cartesian coordinates and the wheel angles, F_x , F_y and M_z , which denotes the traction forces and the traction moment in the body frame separately, can be derived from the geometry relationship of the robot in Figure 2(a) as follows:

$$\begin{aligned} F_x &= \frac{\sqrt{2}}{2} \cdot (-f_1 - f_2 + f_3 + f_4) \\ F_y &= \frac{\sqrt{2}}{2} \cdot (f_1 - f_2 - f_3 + f_4) \\ M_z &= L \cdot (f_1 + f_2 + f_3 + f_4) \end{aligned} \quad (5)$$

where f_i ($i = 1, \dots, 4$) is the traction force acting on the wheel in the direction of the active rolling.

Combining equations (4) and (5), we have the following equations in matrix-vector form as:

$$\mathbf{A} \begin{pmatrix} \dot{V}_x \\ \dot{V}_y \\ \dot{\omega} \end{pmatrix} + m \begin{pmatrix} -V_y \\ V_x \\ 0 \end{pmatrix} \cdot \omega = \mathbf{H} \cdot \mathbf{F}$$

where $\mathbf{A} = \begin{pmatrix} m & 0 & 0 \\ 0 & m & 0 \\ 0 & 0 & I_z \end{pmatrix}$,

$$\mathbf{H} = \begin{pmatrix} -\frac{\sqrt{2}}{2} & -\frac{\sqrt{2}}{2} & \frac{\sqrt{2}}{2} & \frac{\sqrt{2}}{2} \\ \frac{\sqrt{2}}{2} & -\frac{\sqrt{2}}{2} & -\frac{\sqrt{2}}{2} & \frac{\sqrt{2}}{2} \\ L & L & L & L \end{pmatrix}$$

The dynamics of each DC motor can be described as the following equations:

$$L_a \frac{di_a}{dt} + R_a \cdot i_a + k_3 \cdot \omega_m = u \quad (7)$$

$$\mathcal{J}_0 \dot{\omega}_m + f_\mu + \frac{Rf}{n} = k_2 i_a \quad (8)$$

where:

- L_a = the armature inductance.
- i_a = the armature current.
- R_a = the armature resistance.
- k_3 = the electromotive force constant.
- u = the applied armature voltage.
- \mathcal{J}_0 = the combined moment of inertia of the motor, gear train and wheel referred to the motor shaft.
- f_μ = the vicious friction between the ground surface and the wheel.
- n = the gear ratio.
- f = the traction force of the wheels.
- k_2 = the motor torque constant.
- ω_m = the rotate speed of wheel.

Because the electrical time constant of the motor is much smaller than the mechanical time constant, we can neglect dynamics of the motor electric circuit, which leads to:

$$\frac{di_a}{dt} = 0, \quad i_a = \frac{1}{R_a} (u - k_3 \cdot \omega_m) \quad (9)$$

With this assumption, and using the vector notation, the dynamics of the four identical motors can be written as:

$$\mathcal{J}_0 \dot{\Omega}_m + \mathbf{F}_\mu + \frac{R}{n} \mathbf{F} + \frac{k_2 \cdot k_3}{R_a} \Omega_m = \frac{k_2}{R_a} \mathbf{U} \quad (10)$$

where \mathbf{U} is the control input matrix.

Combining expression (3) with equations (6) and (10), we can get the dynamic model of the four-wheeled mobile robot as:

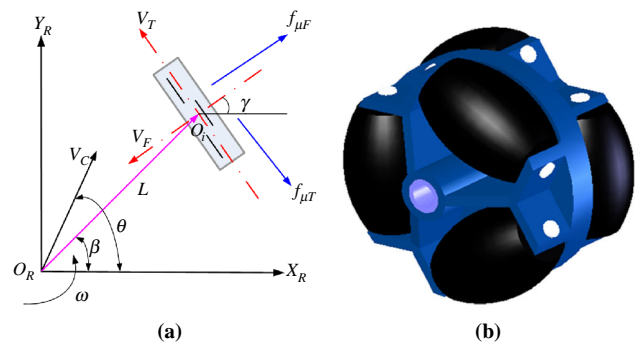
$$\begin{aligned} & \left(\frac{n^2 \cdot \mathcal{J}_0}{R^2} \mathbf{H} \cdot \mathbf{J} + \mathbf{A} \right) \cdot \dot{\mathbf{V}}_R + \frac{n^2 \cdot k_2 \cdot k_3}{R^2 R_a} \mathbf{H} \cdot \mathbf{J} \cdot \mathbf{V}_R + \\ & \frac{n}{R} \mathbf{H} \cdot \mathbf{F}_\mu + m \cdot \begin{pmatrix} -V_y \\ V_x \\ 0 \end{pmatrix} \omega = \frac{k_2 \cdot n}{R_a \cdot R} \cdot \mathbf{H} \cdot \mathbf{U} \end{aligned} \quad (11)$$

3. The amendatory dynamics model with slip

Considering the independent drive of four wheels in our robot which creates one extra DOF and the significant slipping occurred, one exact model and an accurate control method for the robot is required. In this platform, one omni-directional wheel consists of a wheel hub driven by a servo DC motor and a set of rollers that are mounted along the periphery of the wheel hub at a given angle, rotating passively. Therefore, there are two kinds of wheel/ground friction force to be considered. One is the friction force in the wheel hub rolling direction and the other is in the roller rolling direction which is transverse to the former one. And both are the function of velocity in that direction, respectively. Ordinarily, the wheel contact friction forces that are not in the direction of traction force are neglected. But initial trials and analyses with the omni-directional motion indicated that we must also include the latter friction case. As the friction force encountered in these two directions is the slip reason in the running process of motion, especially our OMR running in RoboCup competition where the high acceleration and deceleration motion takes place frequently. Hence, based on the above analysis, this section puts out the improving nonlinear dynamic model including wheel slippage for the OMR.

As shown in Figure 3(a), suppose O_i is the center of i th wheel, the velocity of active hub and passive roller in that wheel is \vec{V}_{T_i} and \vec{V}_{F_i} separately. \vec{V}_{T_i} is perpendicular to \vec{V}_{F_i} based on the structure of the wheel we used here, as shown in Figure 3(b). And suppose O_R is the center of the robot, its speed is defined as $(\vec{V}_C, \vec{\omega})$, where $\vec{\omega}$ is the angular velocity, \vec{V}_C is the translational velocity, and the angle between the vector \vec{V}_C - and X_R -axes is denoted as θ . Besides, the vector directed from O_R to O_i is defined as \vec{L} , the angle between the vector \vec{L}

Figure 3



Notes: (a) Sketch map of the speed direction on one omni-directional wheel; (b) model of the Mecanum wheel

and X_R -axis is denoted as β_i , the angle between the vector \vec{V}_{F_i} and X_R -axis is γ_i , which are confirmed when the robot's structure and installation size is determined. Therefore, we can gain the relationship of above velocity as follows:

$$\begin{aligned} \vec{V}_{O_i} &= \vec{V}_{T_i} + \vec{V}_{F_i} = \vec{V}_C + \vec{V}_\omega \\ \text{where } \vec{V}_\omega &= \vec{\omega} \times \vec{L}, \quad \vec{V}_C = \vec{V}_x + \vec{V}_y \end{aligned} \quad (12)$$

Let \vec{V}_C , \vec{V}_ω , \vec{V}_{T_i} and \vec{V}_{F_i} project to X_R - and Y_R -axes, then we can get the relationship of above velocity as follows:

$$\begin{cases} V_{T_i} = V_c \sin(\gamma_i - \theta) + V_\omega \cos(\beta_i - \gamma_i) \\ V_{F_i} = V_c \cos(\theta - \gamma_i) + V_\omega \sin(\beta_i - \gamma_i) \end{cases} \quad \text{where } (i = 1, \dots, 4) \quad (13)$$

where $\theta = \arctan(V_y/V_x)$ and $\beta_i = \gamma_i = 45^\circ + 90^\circ \cdot (i - 1)$ where $(i = 1, \dots, 4)$ in our platform.

Expanding equation (13) based on the geometry relationship of the robot, we can get such expression ad follows:

$$\begin{cases} \mathbf{V}_T = (v_{T1} \ v_{T2} \ v_{T3} \ v_{T4})^T = \mathbf{H}_T \cdot \mathbf{V}_R \\ \mathbf{V}_F = (v_{F1} \ v_{F2} \ v_{F3} \ v_{F4})^T = \mathbf{H}_F \cdot \mathbf{V}_R \end{cases}$$

$$\text{where } \mathbf{H}_T = \begin{pmatrix} \frac{\sqrt{2}}{2} & -\frac{\sqrt{2}}{2} & L \\ \frac{\sqrt{2}}{2} & \frac{\sqrt{2}}{2} & L \\ -\frac{\sqrt{2}}{2} & \frac{\sqrt{2}}{2} & L \\ -\frac{\sqrt{2}}{2} & -\frac{\sqrt{2}}{2} & L \end{pmatrix} \quad \text{and} \quad (14)$$

$$\mathbf{H}_F = \begin{pmatrix} \frac{\sqrt{2}}{2} & \frac{\sqrt{2}}{2} & 0 \\ -\frac{\sqrt{2}}{2} & \frac{\sqrt{2}}{2} & 0 \\ -\frac{\sqrt{2}}{2} & -\frac{\sqrt{2}}{2} & 0 \\ \frac{\sqrt{2}}{2} & -\frac{\sqrt{2}}{2} & 0 \end{pmatrix}$$

Therefore, following the Newton's law we can get the formulas for friction force as:

$$\mathbf{F}_\mu = \mu_T \cdot \mathbf{V}_T + \mu_F \cdot \mathbf{V}_F \quad (15)$$

where μ_T and μ_F are the friction coefficient in the wheel rotation and transverse direction separately. And μ_F is much less than μ_T due to the design of the omni-directional wheels used here, with smaller friction in the transverse direction than the primary driving direction, owing to the passive rolling cylinders, as shown in Figure 3(b).

Combining expression (11) with expressions (14) and (15), we can get the dynamic model of the four-wheeled OMR with slip as:

$$\begin{aligned} & \left(\frac{n^2 \cdot \mathcal{J}_0}{R^2} \mathbf{H} \cdot \mathbf{J} + \mathbf{A} \right) \cdot \dot{\mathbf{V}}_R \\ & + \left[\frac{n^2 \cdot k_2 \cdot k_3}{R^2 R_a} \mathbf{H} \cdot \mathbf{J} + \frac{n}{R} \mathbf{H} \cdot (\mu_T \cdot \mathbf{H}_T + \mu_F \cdot \mathbf{H}_F) \right] \cdot \mathbf{V}_R \\ & + m \cdot \begin{pmatrix} -V_y \\ V_x \\ 0 \end{pmatrix} \omega = \frac{k_2 \cdot n}{R_a \cdot R} \cdot \mathbf{H} \cdot \mathbf{U} \end{aligned} \quad (16)$$

Define:

$$\begin{aligned} \mathbf{G} &= \frac{n^2 \cdot \mathcal{J}_0}{R^2} \mathbf{H} \cdot \mathbf{J} + \mathbf{A} \\ \mathbf{E} &= \frac{n^2 \cdot k_2 \cdot k_3}{R^2 R_a} \mathbf{H} \cdot \mathbf{J} + \frac{n}{R} \mathbf{H} \cdot (\mu_T \cdot \mathbf{H}_T + \mu_F \cdot \mathbf{H}_F) \end{aligned}$$

and:

$$\mathbf{H}' = \frac{k_2 \cdot n}{R_a \cdot R} \cdot \mathbf{H}$$

as three constant parameter matrix, then expression (16) can be simplified as:

$$\mathbf{G} \cdot \dot{\mathbf{V}}_R + \mathbf{E} \cdot \mathbf{V}_R + m \cdot \begin{pmatrix} -V_y \\ V_x \\ 0 \end{pmatrix} \omega = \mathbf{H}' \cdot \mathbf{U} \quad (17)$$

4. Path-tracking control system based on CTLC

Indeed, in RoboCup competition, the robot moves in a dynamic and oppositional environment, which occurs with high acceleration and deceleration motion frequently, so it cannot be fully compensated for with a simple linear controller, especially for our OMR that slipping is almost inherently encountered in motion. It results in a lack of accuracy. The CTC is a popular technique to achieve tracking control of robot by taking into account dynamic phenomena in the torque computation, via the inverse dynamic model (Khalil and Dombre, 2004; Luh *et al.*, 1980). Following this idea, in this section, we present the CTLC strategy to solve the path-tracking control of a four-wheeled OMR.

First, combining expression (1) with expression (17), we can get the model of the four-wheeled mobile robot as:

$$\mathbf{G} \cdot {}^O_R \mathbf{T}^{-1} \cdot \ddot{\mathbf{X}}_t + \mathbf{E} \cdot {}^O_R \mathbf{T}^{-1} \cdot \dot{\mathbf{X}}_t + m \cdot \begin{pmatrix} -V_y \\ V_x \\ 0 \end{pmatrix} \omega = \mathbf{H}' \cdot \mathbf{U}$$

Which can be simply described as:

$$\mathbf{M}(\mathbf{X}_t) \ddot{\mathbf{X}}_t + \mathbf{C}(\mathbf{X}_t, \dot{\mathbf{X}}_t) \dot{\mathbf{X}}_t = \mathbf{H}' \cdot \mathbf{U} \quad (18)$$

where:

$\mathbf{M}(\mathbf{X}_t)$ = the positive definite inertia matrix.
 $\mathbf{C}(\mathbf{X}_t, \dot{\mathbf{X}}_t)$ = the vector of Coriolis and centrifugal forces.

Suppose that to the feedback controller, one propositional-derivative is used for the closed loop system, and then the control system is as shown in equation (19):

$$M(\mathbf{X}_t)\ddot{\mathbf{X}}_d + C(\mathbf{X}_t, \dot{\mathbf{X}}_t)\dot{\mathbf{X}}_t - M(\mathbf{X}_t)(K_v\dot{e} + K_p e) = \mathbf{H} \cdot \mathbf{U} \quad (19)$$

where:

- \mathbf{X}_d = the trajectory that it is desired to follow.
- $e = \mathbf{X}_t - \mathbf{X}_d$ = the tracking error of the system.
- K_d, K_p = the controller gains are symmetric, positive definite matrices, i.e. $K_v = \text{diag}(k_{v1}, \dots, k_{vn}) > 0$, $K_p = \text{diag}(k_{p1}, \dots, k_{pn}) > 0$, which guarantee the stability of the error system.

Subtract expression (18) from expression (19), and since matrix $M(\mathbf{X}_t)$ is invertible, we can get the resulting dynamics error equation as:

$$\ddot{e} + K_v\dot{e} + K_p e = 0 \quad (20)$$

Which shows that exponential stability of the tracking error e can be guaranteed.

Figure 4 shows the generic representation diagram of the closed-loop motion controller. Path planning gives the desired robot pose, denoted as \mathbf{X}_t at each time sample based on the sensor information fused by omni-directional vision system and odometer data. Inverse kinematics calculates the velocities of the robot, denoted as $\bar{\mathbf{V}}_R$, which are inputs of CTLC. The outputs of the inverse robot dynamics module, the armature voltages of each DC motor, represented as $\bar{\mathbf{U}}$, are used to calculate the velocity of the robot in robot kinematics module. The linearity speed and angular velocity of the robot are fed back via odometer data, and this value is integrated to yield the current robot position and orientation. The velocity errors of the robot compared with their desired value, together with the system's path-tracking error, are the inputs of the CTLC.

5. Simulation and experiment results

5.1 Simulation

The OMR CTLC based on the improving dynamic model including wheel slippage was first verified in Simulink simulation through the experiments which were carried out by considering a circular trajectory as desired paths.

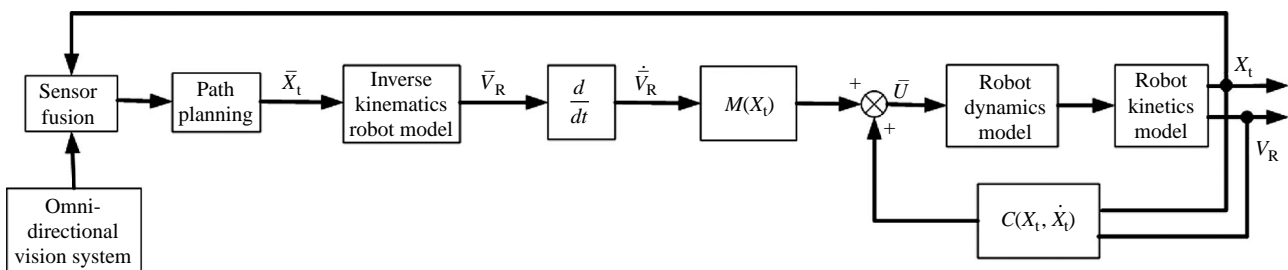
The circular trajectory is obtained by means of the equations:

$$\begin{aligned} x_d(t) &= r_w \sin(\omega t) \\ y_d(t) &= -r_w \cos(\omega t) \end{aligned} \quad (21)$$

where:

- r_w = the radius of the generated circle.
- ω = the angular velocity.

Figure 4 Generic representation diagram of the motion controller



To be as close to the practical effect as possible, all the simulations experiments were carried out by considering a set of physical parameters for the dynamic model of the OMR model (17) given by:

$$\begin{aligned} m &= 20 \text{ kg}, \quad I_z = 0.301 \text{ kgm}^2, \quad R = 0.08 \text{ m}, \\ L &= 0.2125 \text{ m}, \quad n = 14, \quad \mu_T = 0.38, \quad \mu_F = 0.21, \\ R_a &= 1.11 \Omega, \quad k_2 = 36.4 \text{ mNm/A}, \\ k_3 &= 0.0038 \text{ V/rpm}, \quad J_0 = 70.7 \text{ gcm}^2 \end{aligned}$$

And the design parameters involved in the feedback control law equation (20), were considered as:

$$K_p = \begin{pmatrix} 42.5 & 0 & 0 \\ 0 & 36.3 & 0 \\ 0 & 0 & 28.7 \end{pmatrix}, \quad K_v = \begin{pmatrix} 7.5 & 0 & 0 \\ 0 & 6.8 & 0 \\ 0 & 0 & 2.7 \end{pmatrix}$$

With respect to the circular trajectory described in equation (21), it is considered a radius $r_w = 500$ mm and $\omega = 0.8$ rad/s with initial conditions for the mobile robot given by $(x \ y \ \theta \ V_x \ V_y \ \omega) = (0 \ -500 \ 0 \ 0 \ 0 \ 0)$. In Figure 5(a), the velocity errors obtained in the experiment are depicted and the evolution of the circular trajectory on the X-Y plane is shown in Figure 5(b).

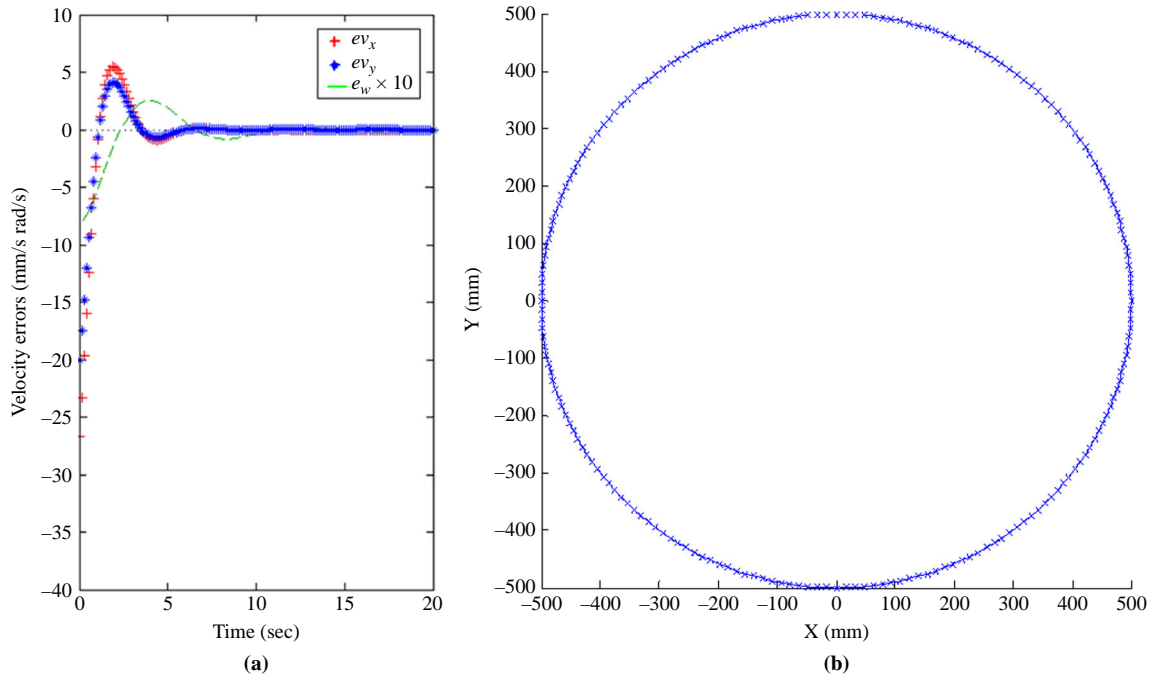
5.2 Experiment

The OMR CTLC based on the improving dynamic model with slip was then tested in a real-time hardware workshop for the robot as shown in Figure 2.

Figure 6 shows the control systems for the OMR. The master controller is composed of a DSP (TI TMS320LF 2407A) and a CPLD (XC95144), used to control the robot velocity and to command the appropriate signal depending on the feedback encoder data to the motor controllers. The DC motor controller is then to control the revolution of every DC motor via the DA value obtained from the master controller and the feedback value achieved from encoder.

In order to check the property of the robot's control system, a pure X-translational motion was commanded in experiment with the speed of $V_x = 1,500$ mm/s and $V_y = \omega = 0$. Figure 7 shows the corresponding x- and y-positions of the robot. In the line of the robot's moving direction, one barricade was erected as an unexpected impact, which was a cube about 10 mm tall. In Figure 7, (a) is the result without considering the effect of slipping; and (b) shows the result based on the improved dynamic model with slip given above. Comparing with these two experimental data, when one

Figure 5 Simulation experiment result



Notes: (a) Robot velocity errors; (b) robot trajectory

Figure 6 Control system for the robot

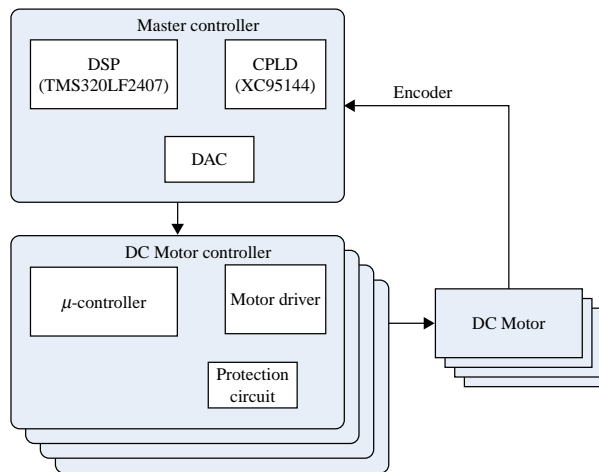
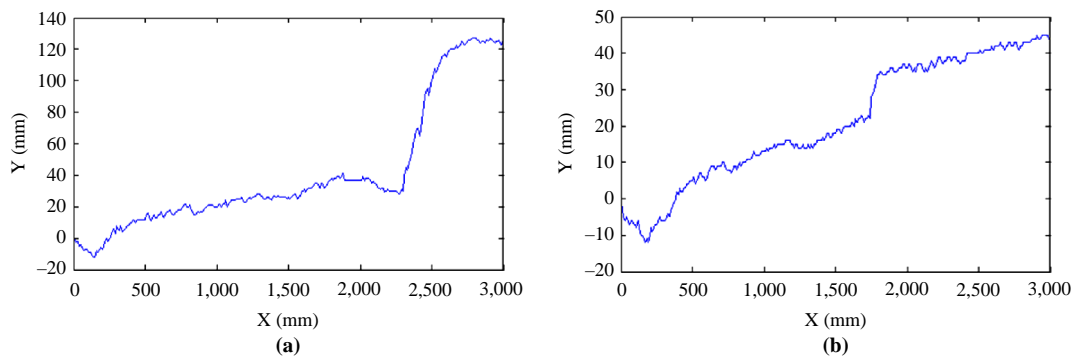


Figure 7 Experiment data of motion



Notes: (a) Experiment data of motion; (b) experiment data of motion

unexpected impact encountered in $x = 2,350$ mm (Figure 7(a)) and in $x = 1,850$ mm (Figure 7(b)), respectively; the result with the new, improved dynamic model with slip showed that the slipping for Y-translational motions was not as severe as the former, which demonstrates the feasibility of our analysis.

6. Conclusion

In this work, a holonomic OMR with four independent driven omni-directional wheels is designed, and the prototype robot is developed. The kinematics and dynamic model of this robot is analyzed. Considering the independent drive of four wheels which creates inevitable slipping in motion, an amendatory dynamics model that includes slipping between the wheels and the motion surface is presented. Based on the above-slipping model, and referring to the well-known computer torque control strategy, one CTLC system is implemented in order to solve the path-tracking problem associated to the robot. An acceptable performance of the dynamic model and the control strategy is shown by means of simulation and experiments.

References

- Cao, Q., Huang, Y. and Leng, C. (2007), "An amendatory dynamic model with slip for four-wheeled omnidirectional mobile robot", *Proceedings of the SPIE – The 2007 International Conference on Mechatronics and Information Technology (ICMIT2007) on Mechatronics, MEMS, and Smart Materials*, Vol. 6794, pp. 7945-50.
- Carter, B., Good, M., Dorohoff, M., Lew, J., Williams, R.L. II and Gallina, P. (2001), "Mechanical design and modeling of an omni-directional robocup player", *Proceedings of the RoboCup 2001 International Symposium, Seattle, WA*.
- de Wit, C.C. and Roskam, R. (1991), "Path following of a 2-DOF wheeled mobile robot under path and input torque constraints", *Proceedings of the IEEE International Conference on Robotics and Automation*, Vol. 2, pp. 1142-7.
- Dixon, W.E., Dawson, D.M., Zergeroglu, E. and Zhang, F. (2000), "Robust tracking and regulation control for mobile robots", *International Journal of Robust and Nonlinear Control*, Vol. 10, pp. 199-216 (special issue on control of underactuated nonlinear systems).
- Do, K.D., Jiang, Z. and Pan, J. (2004), "A global output-feedback controller for simultaneous tracking and stabilization of unicycle-type mobile robots", *IEEE Transactions on Robotics and Automation*, Vol. 20 No. 2, pp. 589-94.
- Driessen, B.J. (2006), "Adaptive global tracking for robots with unknown link and actuator dynamics", *International Journal of Adaptive Control and Signal Processing*, Vol. 20 No. 3, pp. 123-38.
- He, Z.F., Lin, L.F. and Ma, X.Y. (2004), "Design, modeling and trajectory generation of a kind of four wheeled omnidirectional vehicle", *IEEE International Conference on Systems, Man and Cybernetics*, Vol. 7, pp. 6125-30.
- Khalil, W. and Dombre, E. (2004), *Modeling, Identification and Control of Robots*, Elsevier, London.
- Liu, Y., Wu, X., Zhu, J. and Lew, J. (2003), "Omni-directional mobile robot controller design by trajectory linearization", *Proceedings of the American Control Conference*, Vol. 4, pp. 3423-8.
- Luh, J., Walker, M. and Paul, R. (1980), "Resolved acceleration control of mechanical manipulators", *IEEE Transactions on Automatic Control*, Vol. 25 No. 3, pp. 468-74.
- Muir, P.F. and Neuman, C.P. (1987a), "Kinematic modeling for feedback control of an omnidirectional wheeled mobile robots", *IEEE International Conference on Robotics and Automation*, pp. 1772-8.
- Muir, P.F. and Neuman, C.P. (1987b), "Kinematic modeling of wheeled mobile robots", *Journal of Robotic Systems*, Vol. 4 No. 2, pp. 281-340.
- Myung, J.J., Kim, H.S., Kim, S. and Kim, J.H. (2000), "Omni-directional mobile base OK-II", *IEEE International Conference on Robotics and Automation*, Vol. 4, pp. 3449-54.
- Nobuhiro, U., Kazuhiro, T. and Motoji, Y. (2007), "A study of safety control for omni-directional mobile robots in consideration of driving wheel slips", *Proceedings of the 13th IASTED International Conference on Robotics and Applications*, pp. 27-32.
- Pin, F.G. and Killough, S.M. (1994), "A new family of omni-directional and holonomic wheeled platforms for mobile robots", *IEEE Transactions on Robotics and Automation*, Vol. 10 No. 4, pp. 480-9.
- Sarkar, N., Yun, X. and Kumar, V. (1994), "Control of mechanical systems with rolling constraints: application to dynamic control of mobile robots", *International Journal of Robotics Research*, Vol. 13 No. 1, pp. 55-69.
- Shing, C.-C., Hsu, P.-L. and Yeh, S.-S. (2006), "T-S fuzzy path controller design for the omnidirectional mobile robot", *Proceedings of the 2006 IEEE Industrial Electronics Conference IECON*, pp. 4142-7.
- Tsai, C.C. and Wang, T.S. (2005), "Nonlinear control of an omnidirectional mobile robot", *Proceedings of the 8th International Conference on Automation Technology*, pp. 727-32.
- Vazquez, J.A. and Velasco-Villa, M. (2007), "Computed-torque control of an omnidirectional mobile robot", *ICEEE 2007 4th International Conference on Electrical and Electronics Engineering*, pp. 274-7.
- Wada, M. (2005), "An omnidirectional 4WD mobile platform for wheelchair applications", *Proceedings of the IEEE/ASME International Conference on Advanced Intelligent Mechatronics (AIM2005)*, pp. 576-81.
- Watanabe, K., Shiraishi, Y., Tzafestas, S., Tang, J. and Fukuda, T. (1998), "Feedback control of an omnidirectional autonomous platform for mobile service robots", *Journal of Intelligent and Robotic Systems*, Vol. 22 Nos 3/4, pp. 315-30.
- Williams, R.L. II, Carter, B.E., Gallina, P. and Rosati, G. (2002a), "Dynamic model with slip for wheeled omnidirectional robots", *IEEE Transactions on Robotics and Automation*, Vol. 18 No. 3, pp. 285-93.
- Williams, R.L. II, Carter, B.E., Gallina, P. and Rosati, G. (2002b), "Wheeled omni-directional robot dynamics including slip", *Proceedings of the ASME Design Engineering Technical Conference (DETC2002)*, Vol. 5A, pp. 201-7.
- Witus, G. (2000), "Mobility potential of a robotic 6-wheeled omni-directional drive vehicle (ODV) with z-axis and tire inflation control", *Proceedings of the SPIE – The International Society for Optical Engineering*, Vol. 4024, pp. 106-14.

Further reading

- Isidori, A. (1995), *Nonlinear Control Systems*, 3rd ed., Springer, New York, NY.
- Nagy, T.K., D’Andrea, R. and Ganguly, P. (2004), “Near-optimal dynamic trajectory generation and control of an omnidirectional vehicle”, *Robotics and Autonomous Systems*, Vol. 47 No. 1, pp. 47-64.
- Nagy, T.K., Ganguly, P. and D’Andrea, R. (2002), “Real-time trajectory generation for omni-directional vehicle”, *Proceedings of the American Control Conference*, pp. 286-91.

- Samani, H.A., Abdollahi, A., Ostadi, H. and Rad, S.Z. (2004), “Design and development of a comprehensive omnidirectional soccer robot”, *International Journal of Advanced Robotic Systems*, Vol. 1 No. 3, pp. 191-200.
- Wu, J. (2005), “Dynamic path planning of an omnidirectional robot in a dynamic environment”, PhD dissertation, Ohio University, Athens, OH.

Corresponding author

Yanwen Huang can be contacted at: ywhuang@sjtu.org